# Supporting Information

Li *et al.* 10.1073/pnas.0802876105

## SI Materials and Methods

**Generation of M*ef2c* Conditional Null Mice and MEF2 Reporter Mice.** We crossed mice expressing the nestin-*Cre* transgene (*n-Cre*$^{+}$) (1) with mice carrying the conventional exon 2-deleted allele of *Mef2* (*Mef2c*$^{\Delta 2}$) (2) to generate *n-Cre*$^{+}$/*Mef2*$^{+/\Delta 2}$ mice. These mice were then crossed with *Mef2c*$^{loxp/loxp}$ mice (3) to obtain the *n-Cre*$^{+}$/*Mef2c*$^{loxp/\Delta 2}$ conditional null mice. We defined as embryonic day 0.5 (E0.5) the day a vaginal plug was detected; the day of birth is indicated as P0. The MEF2 reporter mice, comprising transgenic mice harboring a *lacZ* reporter gene controlled by a MEF2-dependent promoter, have been described previously (4).

**Quantitative Immunohistochemistry for Neural Stem/Progenitor Cells (NSCs) and Neuronal Markers.** Mouse brains were dissected in PBS and fixed in 4% paraformaldehyde at 4°C overnight. Cryostat sections of 30-$\mu$m thickness were collected in PBS for free-floating immunohistochemistry. Epitope retrieval was performed in citrate buffer containing 10 mM sodium citrate and 0.05% Tween 20 at pH 6.0. The following primary antibodies were used: $\beta$-galactosidase (AB1211; Chemicon), Ki67 (VP-K451; Vector Laboratories), TuJ1 (MMS-435P or PRB-435P; Covance), nestin (MAB353; Chemicon or AF2736; R&D), DCX (AB5910; Chemicon), NeuN (MAB377B; Chemicon), Er81 (PRB-362C-100; Covance), Tbr1 (AB9616; Chemicon), GAD 65/67 (AB1511; Chemicon), NCAM (C-9672; Sigma), Dab-1 (GTX27522; GeneTex), p35 (2673; Cell Signaling), BLBP (AB9558; Chemicon), MAP-2 (AB5622; Chemicon), vimentin (AB5733; Chemicon), NR1 (05-432; Upstate), BrdU (OBT0030CX; Accurate), and integrin $\alpha$5 (AB1928; Chemicon). Immunofluorescent signals were enhanced with TSATM Plus (PerkinElmer). By using the SlideBook software package (Intelligent Imaging Innovations), fluorescence intensities were measured along five uniformly chosen lines within each band across a section (indicated by the white rectangular "area of interest"). The measured regions allowed us to compare quantitatively the difference between control and *Mef2c*-null mice with respect to various markers observed within the cortical plate. Fluorescence intensities (mean ± SEM) from 90 binned points were plotted across each section as a percentage of the total intensity within that region. A two-way ANOVA was used to calculate the mean square residuals, which were then compared statistically by post hoc analysis (significance taken as $P < 0.001$). Although the entire section was analyzed in this fashion, only bands with the most highly significant statistical differences between null and control are illustrated here.

**Stereological Neuronal Cell Counts.** The ratio of (BrdU-positive + NeuN-positive)/total BrdU-positive cells was taken as an index of neurogenesis during development compared for control and *Mef2c*-null mice. For each mouse and immunostain, three serial sections (30 $\mu$m in thickness) of corresponding brain regions were analyzed. We used deconvolution microscopy and a modified version of the optical dissector technique to quantify neuronal cells with the SlideBook software package, as we have described in ref. 2. For adults, the total number of NeuN-positive neuronal cells was counted in the cortex using the optical dissector.

**Quantitative Immunohistochemical Analysis for Volume of Dendritic Neuropil and Synapse Number.** Using a 40× objective lens and a constant exposure time, *z* stacks of images (*z* step size of 0.5 $\mu$m) were obtained from nine randomly selected CA1 regions of the hippocampus per animal. The image stacks were subjected to constrained iterative deconvolution, and regions occupied by neuronal cell bodies were removed from the analysis. The volume of neuropil occupied by MAP-2-labeled processes or synaptophysin-labeled presynaptic terminals was calculated as the ratio of fluorescent to total voxels from the best focused planes of each image stack. Image stack acquisition, threshold segmentation, and volume calculations were performed by an observer blinded to genotype.

**Electrophysiological Techniques.** Mice were deeply anesthetized and decapitated. The brains were rapidly removed and placed into ice-cold sucrose-substituted artificial cerebrospinal fluid (aCSF) gassed with 95% $O_2$ and 5% $CO_2$. Brains were dissected and sectioned on a Vibratome (Leica VT 1000S) transversely with respect to the longitudinal axis for hippocampal slices (400 $\mu$m thick) or coronally for neocortical slices. For multielectrode array (MEA) recordings, slices were positioned in the chamber (MEA-60; Multi Channel Systems) at least 1 h before use and superfused with aCSF at 32°C for the duration of the experiment. For patch–clamp recordings, either adult or early postnatal (P0–P4) slices were superfused with aCSF at room temperature, and voltage–clamp recordings performed in the whole-cell configuration. Layer 5 cortical neurons were visualized using an upright infrared-DIC-video-microscope with a 40× water-immersion objective (Axioskop; Carl Zeiss). Responses to exogenous NMDA were recorded in the nominal absence of extracellular $Mg^{2+}$. We recorded AMPA receptor-mediated evoked EPSCs at a holding potential of -70 mV in aCSF in the presence of 30 $\mu$M bicuculline to block $GABA_A$ receptors and 50 $\mu$M D-(−)-2 amino-5-phosphonovaleric acid (D-APV) to block NMDA receptors. For mEPSCs, 1 $\mu$M tetrodotoxin was added to the medium, steady-state was reached, and analysis was performed with the Mini Analysis program (Version 6.0.3; Synaptosoft).

**Behavioral Tests.** ***Elevated plus maze.*** This apparatus has four arms (5 × 30 cm) at right angles to each other and is elevated 30 cm from the floor. Two of the arms have 16-cm-high walls (enclosed arms), and two arms have a 0.5-cm lip, but no walls (open arms). Mice were placed onto the center of the maze and allowed free access to all four arms for 5 min. Behavior was video recorded, and the time spent on each arm was scored blind. Percentage of time spent on the open arms and number of arm entries are calculated.

***Locomotor activity.*** Locomotor activity was measured in polycarbonate cages (42 × 22 × 20 cm) placed into frames (25.5 × 47 cm) mounted with two levels of photocell beams at 2 and 7 cm above the bottom of the cage (San Diego Instruments). These two sets of beams allowed for the recording of both horizontal (locomotion) and vertical (rearing) behavior. A thin layer of bedding material was applied to the bottom of the cage. Mice were tested for 30 min.

***Cued and contextual fear conditioning.*** In this test, mice learn to associate a novel environment (context) and a previously neutral stimulus (conditioned stimulus, a tone) with an aversive foot shock stimulus. Testing then occurs in the absence of the aversive stimulus. Freezing responses can be triggered by exposure to either the context in which the shock was received (context test) or the conditioned stimulus (CS+ test). Conditioning took place in a Freeze Monitor chamber (San Diego Instruments) housed in a soundproofed box. The conditioning chamber (26 × 26 ×

17 cm) was made of Plexiglass with a speaker and light mounted on two opposite walls. The chamber was installed with a shockable grid floor. On day 1, mice were placed in the conditioning chamber for 10 min to habituate them to the apparatus. On day 2, the mice were exposed to the context and conditioned stimulus (30 s, 3,000 Hz, 80-dB sound) in association with foot shock (0.70 mA, 2 s, scrambled current). Specifically, a 5.5-min session was run in which the mice received two shock exposures, both in the last 2 s of a 30-s tone exposure. On day 3, contextual conditioning (as determined by freezing behavior) was measured in a 5-min test in the chamber where the mice were trained (context test). Two to four hours after this test, the mice were tested for cued conditioning (CS+ test). During this test, the mice were placed in a novel context for 3 min, after which they were exposed to the conditioned stimulus (tone) for 3 min. For this test, the chamber was disguised with new walls (black opaque plastic creating a triangular-shaped compartment in contrast to a clear plastic square compartment), a new floor (black opaque plastic in contrast to metal grid), and a novel odor (drop of orange extract under the floor). Freezing behavior, i.e., the absence of all voluntary movements except breathing, was measured in 5-min intervals in three sessions (habituation, conditioning, and context test) or in 3-min intervals in the CS+ test by a validated computer-controlled recording of photocell beam interruptions. Freezing behavior in each test is indicative of the formation of an association between the particular stimulus (either the environment or the tone) and the shock, showing that learning has occurred.

***Y maze.*** A single 5-min test was performed in which each mouse was placed in the center of the Y. Arm entries were recorded by video camera, and the total number of arm entries and the order of entries were determined. Spontaneous alternations were defined as consecutive triplets of different arm choices.

***Novel object exploration.*** This test was conducted in an open-field apparatus (79 × 79 × 50.8 cm) with a small bottle placed in one location for four 5-min trials. For the fifth trial, the object was moved to a different spatial location. The intertrial interval was 1 min. All behavior was video recorded and then scored for object contact time (touching with nose or nose pointing at object and within 0.5 cm of object).

***Paw clasping.*** Paw-clasping behavior was noticed during handling and was not seen while the mice were in their normal cage environment. For measurements, mice were picked up by the distal third of their tails and observed for 10 s. Ratings were given based on clasping of the front and/or back paws: 0, no paw clasping; 1, occasional clasping of front paws (limited clasping); and 2, constant clasping of front paws and occasional clasping of back paws.


1. Tronche F, *et al.* (1999) Disruption of the glucocorticoid receptor gene in the nervous system results in reduced anxiety. *Nat Genet* 23:99–103.
2. Lin Q, *et al.* (1997) Control of mouse cardiac morphogenesis and myogenesis by transcription factor MEF2C. *Science* 276:1404–1407.
3. Vong LH, Ragusa MJ, Schwarz JJ (2005) Generation of conditional *Mef2c*$^{loxp/loxp}$ mice for temporal- and tissue-specific analyses. *Genesis* 43:43–48.
4. Naya FJ, *et al.* (1999) Transcriptional activity of MEF2 during mouse embryogenesis monitored with a MEF2-dependent transgene. *Development* 126:2045–2052.

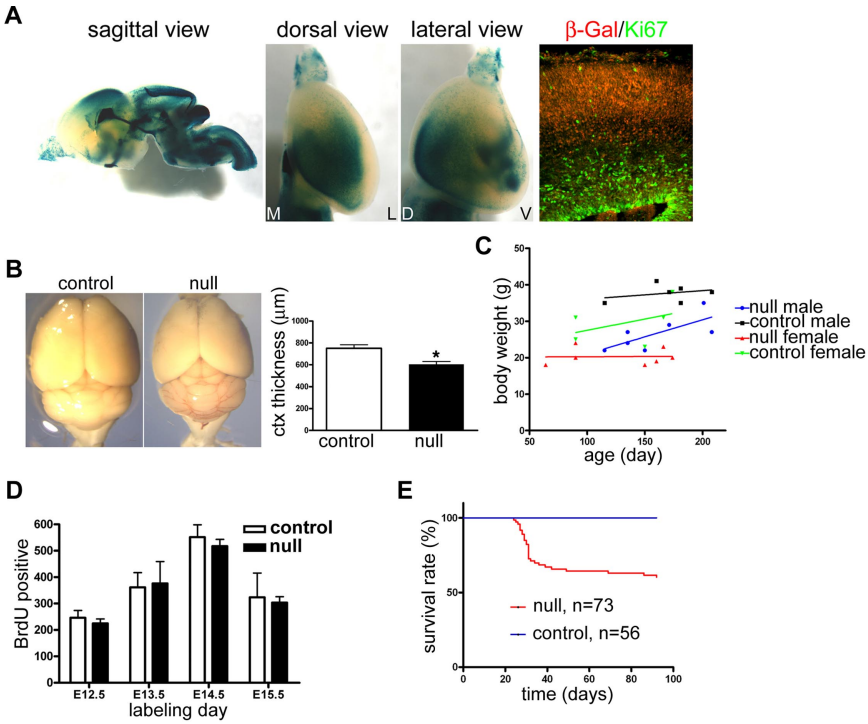


**Fig. S1.** Pattern of MEF2 transcriptional activity in WT and *Mef2c*-null mouse brain. (*A*) β-Galactosidase staining represents MEF2 transcriptional activity in transgenic mice harboring a *lacZ* reporter gene controlled by a MEF2-dependent promoter (4). At E18.5, MEF2 transcriptional activity is present in multiple brain regions. In cerebrocortex, MEF2 transcriptional activity is distributed in a rostral-low to caudal-high gradient and restricted to postmitotic neurons that are negative for the proliferative marker Ki67. (*B*) Smaller adult brain cortex size and reduced thickness of neocortex of *n-Cre*$^{+}$/*Mef2c*$^{loxp/\Delta 2}$ conditional null mice. (*C*) Reduced body weight in *n-Cre*$^{+}$/*Mef2c*$^{loxp/\Delta 2}$ mice. (*D*) BrdU labeling at various embryonic ages shows no difference in proliferation of neural progenitors between control and *n-Cre*$^{+}$/*Mef2c*$^{loxp/\Delta 2}$-null mice. (*E*) Kaplan–Meier curve demonstrates lower survival rate of *n-Cre*$^{+}$/*Mef2c*$^{loxp/\Delta 2}$-null mice.

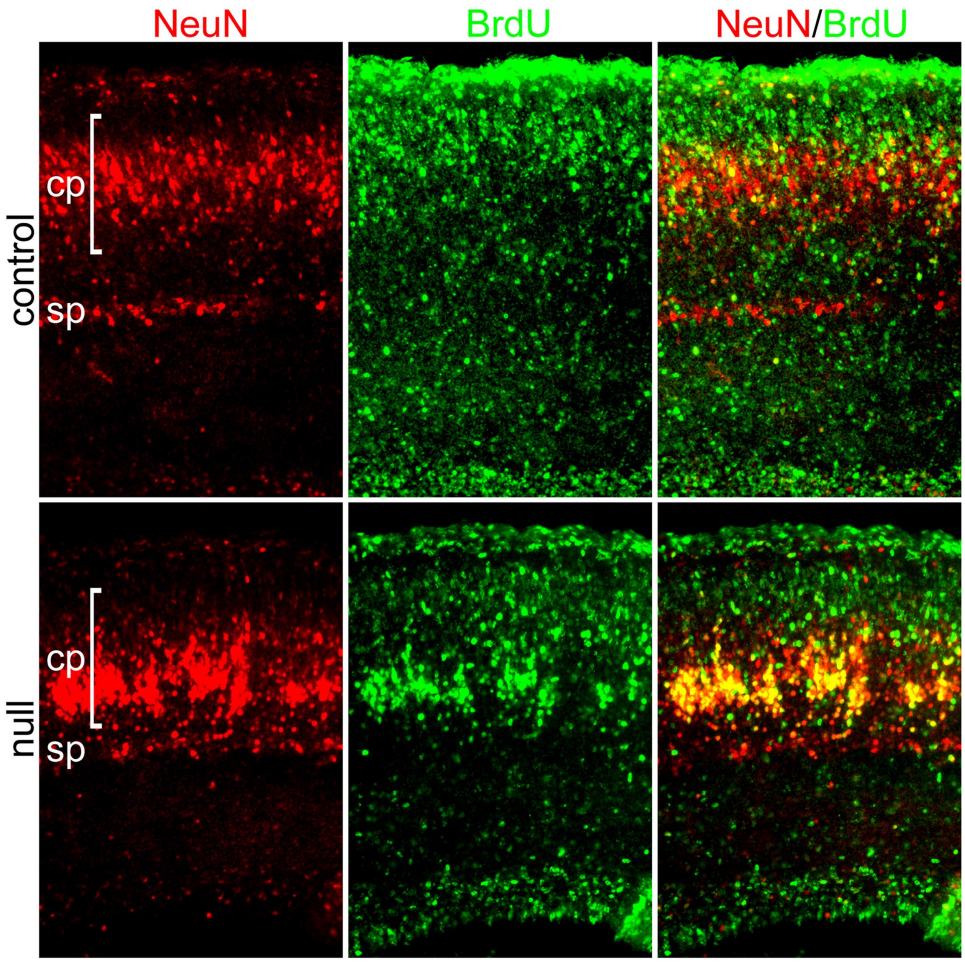


**Fig. S2.** In *Mef2c*-null mice, BrdU-labeled neurons born at E14.5 migrated abnormally without affecting expression of the mature neuronal marker NeuN. Cp, cortical plate; sp, subplate

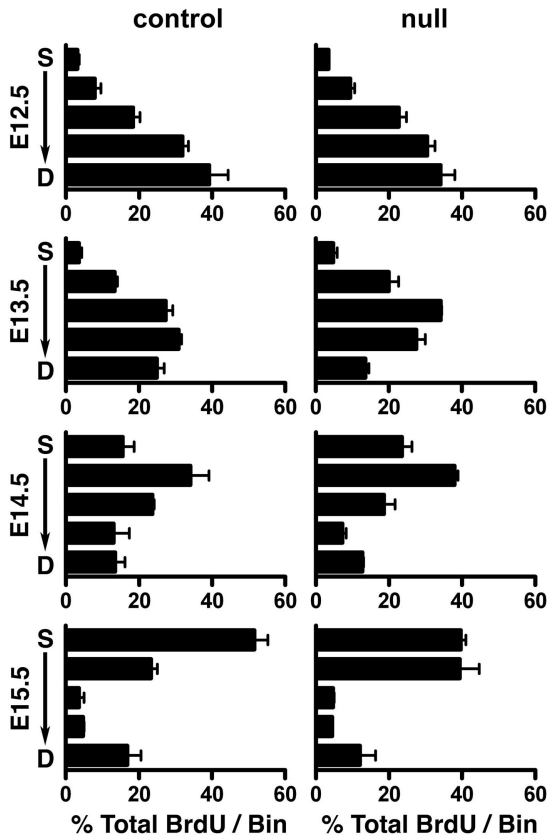


**Fig. S3.** Birthdating experiment shows that the order of layer formation is normal in *Mef2c*-null mice. The graphs for each age group represent the percentage of total BrdU-positive cells in the neocortex in five layers from superficial (S) to deep (D). Values are mean ± SEM; $n = 11$ for control [*Mef2c*(+/Lox)] mice; $n = 12$ for conditional null mice [*Mef2c*(−/NKO), where NKO = nestin-*Cre*/*Mef2c* knockout].

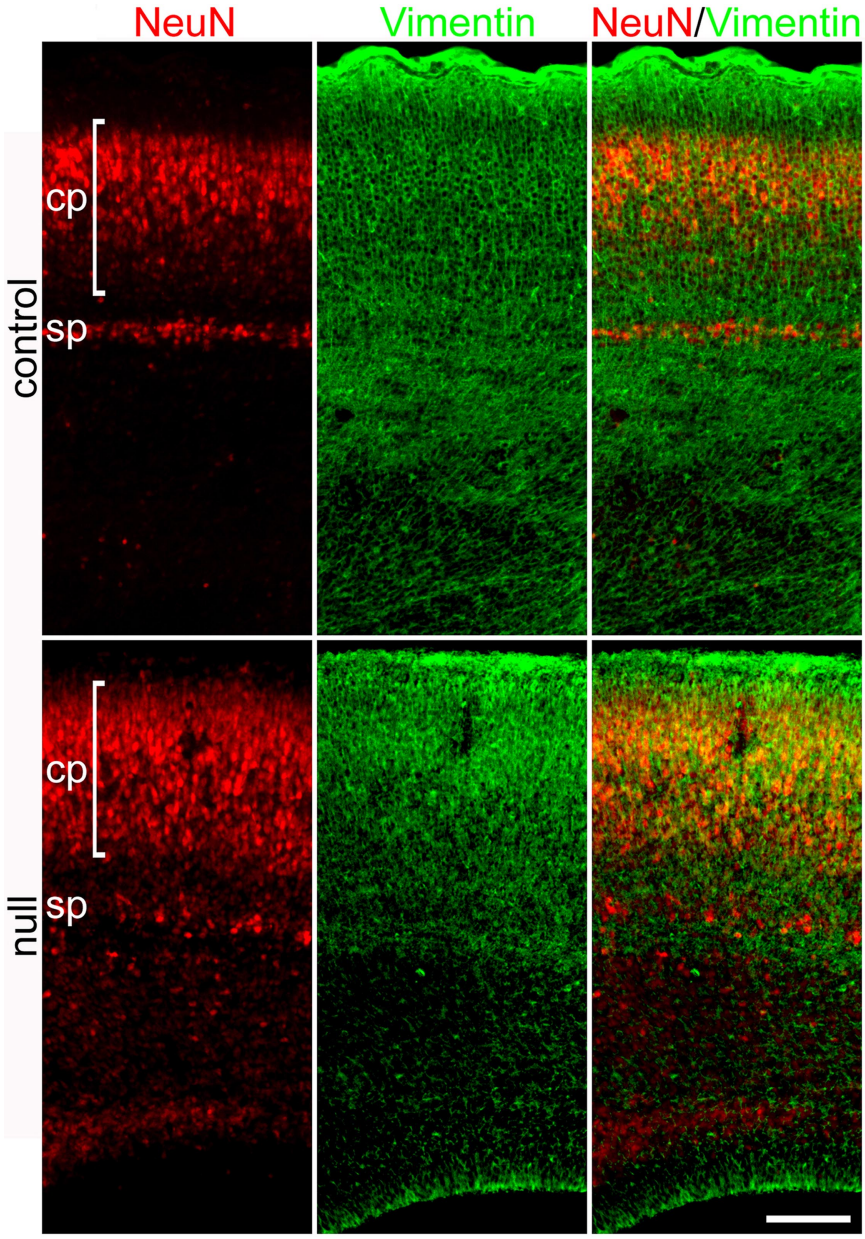


**Fig. S4.** Radial glia in the mildly affected E18.5 *Mef2c*-null phenotype. Radial glia (labeled here by vimentin) manifested subtle alterations in the neocortex with a pattern similar to that of NeuN-stained migrating neurons.

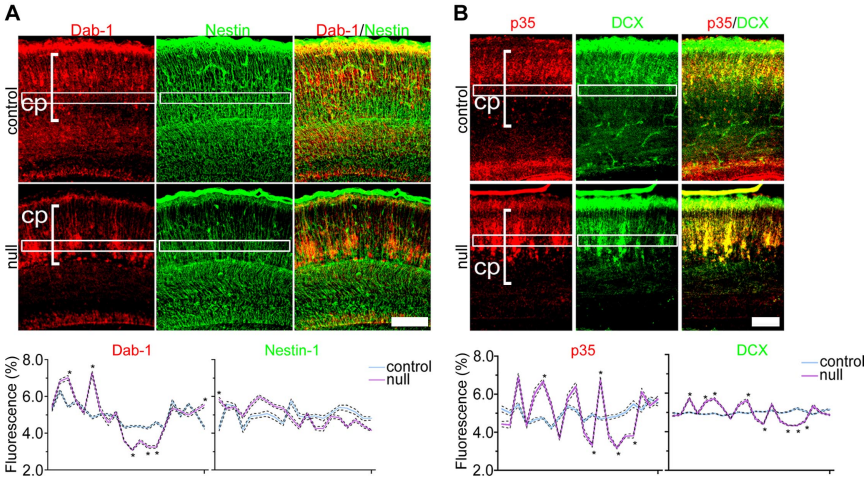


**Fig. S5.** Despite the severe *Mef2c*-null cortical phenotype, genes known to regulate cell migration were expressed at E18.5. (*A*) *Mef2c*-null neurons expressed the Reelin signaling protein Disabled-1 (Dab-1). Nestin staining shows that the distribution of NSCs was normal. (*B*) DCX-positive *Mef2c*-null neurons expressed p35 (CDK5 signaling). (Scale bars, 100 $\mu$m.) Graphs quantify immunofluorescent staining in control vs. *Mef2c* nulls (*, $P < 0.001$) to highlight the fact that migration markers track with the committed neuronal markers (compare with graph in Fig. 2*A*).

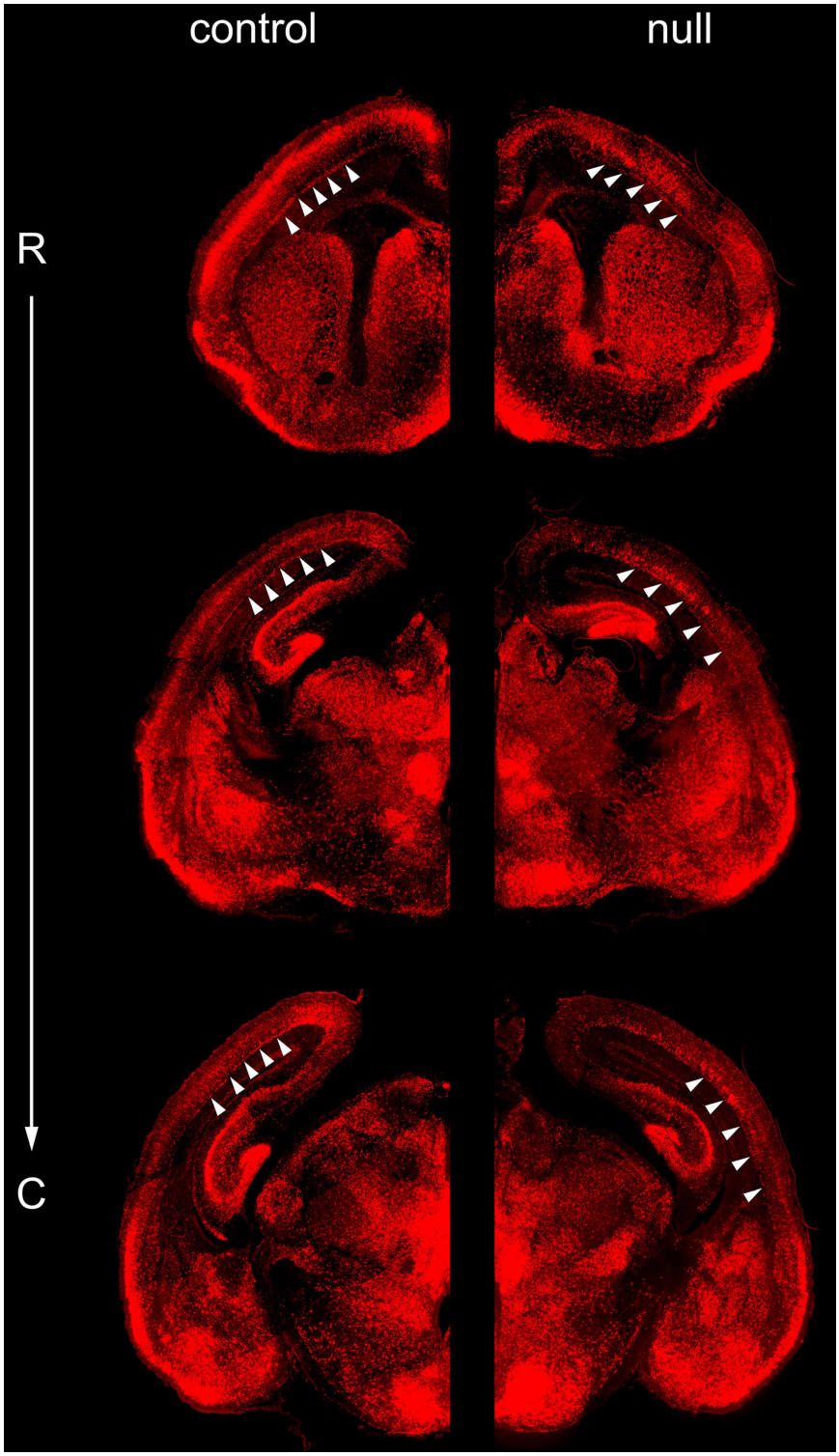


**Fig. S6.** Severe neuronal migratory deficit in the *Mef2c* conditional null is demonstrated with NeuN staining of rostral (R) to caudal (C) brain sections at E18.5. Arrowheads indicate the location of the subplate.

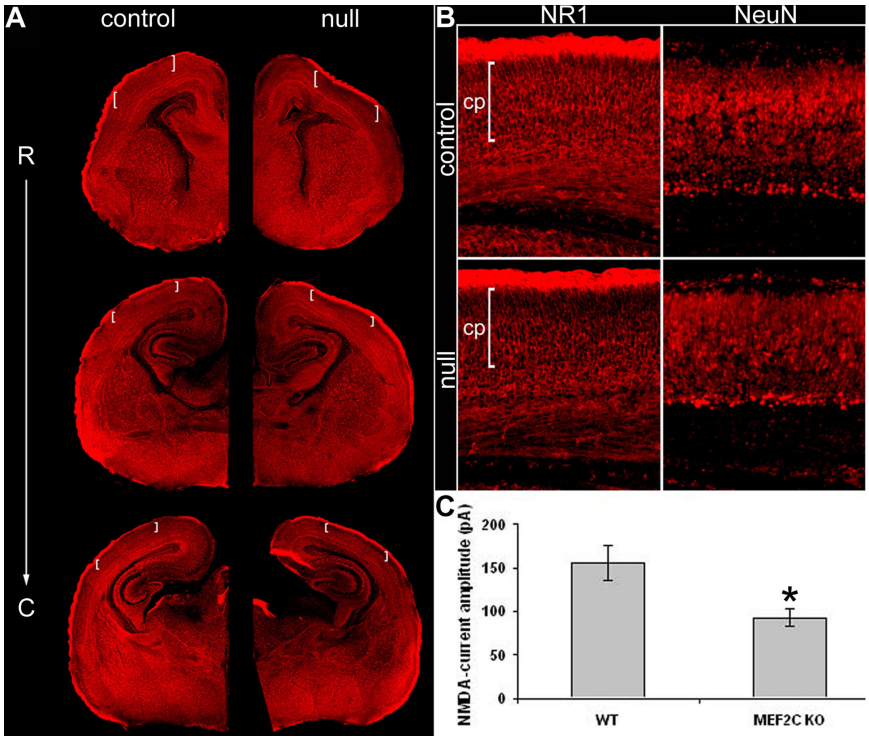


**Fig. S7.** Decrease in NMDA receptor expression and activity in the perinatal cerebrocortex of *Mef2c*-null mice. (*A*) Decrement in NMDA receptor subunit NR1 expression in the neocortex observed from rostral (R) to caudal (C) in brain sections obtained at E18.5 from *Mef2c* conditional null versus control mice. Decreased NR1 immunostaining was particularly evident in the more superficial layers of the cortex (delineated by white brackets). Quantitative deconvolution microscopy using SlideBook software demonstrated an ≈35% decrement in NR1 staining ($n = 4$; $P < 0.02$, *t* test). (*B*) Higher magnification under deconvolution microscopy to show that NR1 staining was decreased in the cortical plate of *MEF2c*-null mice versus control, whereas NeuN staining (for mature neurons) was relatively unaffected. (*C*) NMDA (30 $\mu$M)-induced responses from layer 5 neocortex monitored by whole-cell recording with patch electrodes at P0–P4. Approximately a 40% decrease in NMDA responses was observed in *Mef2c* conditional null versus control mice ($n = 19$, $P < 0.003$, *t* test).

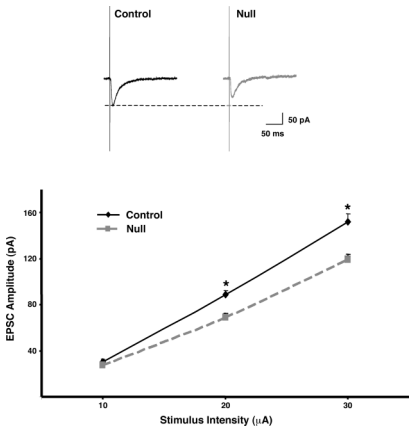


**Fig. S8.** Representative traces of evoked EPSCs from single cortical neurons recorded in layer 5 of acute cortical slices. Input/output (I/O) curves of EPSC amplitude recorded at two different stimulus strengths show that evoked EPSCs of control mice were significantly larger than those of *Mef2* nulls ($P < 0.005$).

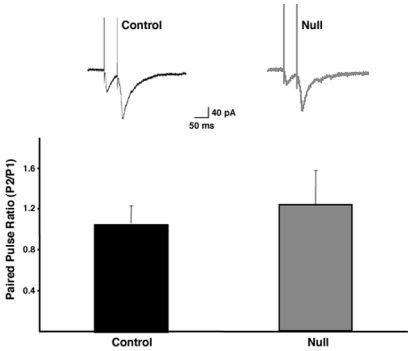


**Fig. S9.** Representative paired pulse facilitation (PPF). The pulse ratios of control and *Mef2c*-null mice were not significantly different but revealed a trend toward increased PPF in the nulls. Stimulus interpulse interval, 50 ms ($n \geq 4$ for each group). Values are mean ± SEM.

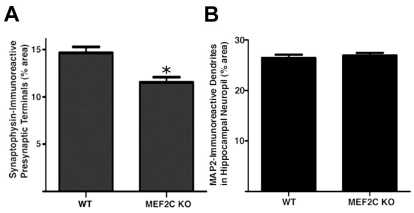


**Fig. S10.** Decreased synapse number in adult *Mef2c* conditional null mice versus control. Synaptophysin immunostaining for presynaptic sites was quantified by deconvolution microscopy (see *SI Materials and Methods*) and found to be significantly reduced in *Mef2c* null versus WT mice ($n = 6$, $P > 0.002$, $t$ test). In contrast, MAP-2 staining was not different between the two genotypes.

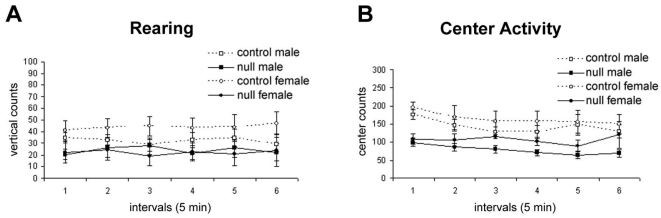


**Fig. S11.** Rearing behavior (*A*) and center activity (*B*) measures in *Mef2c*-null mice suggest an increased anxiety level. Mice lacking MEF2C spent less time in the center of the cage ($P < 0.001$) and showed a trend ($P = 0.06$) towards decreased rearing behavior. This is consistent with the notion that an increased level of anxiety accounted for their avoidance of the more open area and decreased vertical exploration. Values are mean ± SEM, $n \geq 10$ animals tested in each group.